

# Straightforward computation of high-pressure elastic constants using Hooke's law: A prototype of metal Ru

Zhong-Li Liu\*

*College of Physics and Electric Information, Luoyang Normal University, Luoyang 471934, China*

Xiu-Lu Zhang

*Laboratory for Extreme Conditions Matter Properties,  
Southwest University of Science and Technology, 621010 Mianyang, China*

Cuan-Cuan Zhu

*College of Physics and Electric Information, Luoyang Normal University, Luoyang 471934, China and  
School of Materials Science and Engineering, Henan Polytechnic University, Jiaozuo 454000, China*

Hai-Yan Wang<sup>†</sup>

*School of Materials Science and Engineering, Henan Polytechnic University, Jiaozuo 454000, China*

In this paper, we did a systematic comparative study on the accuracy of two computational methods of elastic constants combined with the density functional theory (DFT), the stress-strain method and the energy-strain method. We took metal Ru as a prototype to compare its high-pressure elastic constants calculated by our present stress-strain method with the previous energy-strain results by others. Although the two methods yielded almost the same accuracy of high-pressure elastic constants for Ru, our stress-strain method directly based on the Hooke's law of elasticity theory is much straightforward and simple to implement. However, the energy-strain method needs complicated pressure corrections because of the pressure effects on the total energy. Various crystal systems have various pressure correction methods. Hence, the stress-strain method is preferred to calculate the high-pressure elastic constants of materials. Furthermore, we analyzed the variations of the elastic moduli, elastic anisotropy, sound velocities, Debye temperature of Ru with pressure.

## I. INTRODUCTION

Elastic constants are key parameters for us to understand the physical and even chemical properties of materials. They correlate closely with various physical properties, such as mechanical (hardness)<sup>1</sup>, thermodynamic<sup>2</sup>, melting<sup>3</sup>, acoustic<sup>4</sup>, and so on. Elastic constants are frequently used in many fields, including materials science, physics, geophysics, chemical, condensed matter, and engineering and technology. Hence, the elastic properties of materials continue attracting much attention from researchers.

There are generally two methods used for calculating the second-order elastic constants of materials. One is the strain-energy method based on the relationship between specific energy and strain magnitude<sup>2,5-9</sup>. The other is the stress-strain method<sup>2,10,11</sup> fundamentally based on the Hooke's law of elasticity theory. The two methods combined with the state-of-the-art density functional theory (DFT) make the calculations of elastic constants simple. At zero pressure, the two methods both easily yield identical results; however, at high pressure the energy-strain method needs complex pressure corrections<sup>5,7</sup> to achieve effective elastic constants, with different correction formulas for different crystal systems<sup>7</sup>. While, at high pressure the stress-strain method is still straightforward and simple without pressure corrections, directly according to the Hooke's

law like the case of zero pressure.

In this paper, we have a comparative study on the two methods in the calculations of high-pressure elastic constants of materials. We here take metal Ru as the prototype to compare the results of the two methods combined with DFT. Since the high-pressure elastic constants of Ru has already been calculated using the energy-strain method with pressure corrections by Lugovskoy et al.<sup>12</sup>. We only re-calculated its high-pressure elastic constants using the stress-strain method. The details of computational algorithm are introduced in Ref.<sup>13</sup>, and our recently developed ElasTool package<sup>14</sup> was used to calculate the elastic constants of Ru. We find that our stress-strain method yielded the identical high-pressure elastic constants of Ru, compared to the previous energy-strain method<sup>12</sup>.

## II. COMPUTATIONAL DETAILS

The original Hooke's law states that the force ( $F$ ) exerted on a spring is linearly proportional to the spring's deformation magnitude ( $x$ )—that is,  $F = kx$ , where  $k$  is a proportional coefficient reflecting its stiffness, and  $x$  is small compared to the possible maximum deformation of the spring. The modern elasticity theory extends Hooke's law to state that the strain (deformation) of a crystal is proportional to the stress applied to it. However, since general stresses and strains are tensors, the proportional

coefficient is no longer just a single number, but rather a tensor represented by a matrix.

### A. Elastic constants computation method

According to Hooke's law, within the linear elastic regime of a crystal the relation between the stresses  $\sigma_i$  and its induced strains  $\varepsilon_j$  is,

$$\sigma_i = \sum_{j=1}^6 C_{ij} \varepsilon_j \quad (1)$$

where the  $C_{ij}$  are the elastic constant of the crystal.

We can obtain all the elastic constants of a material from Eq.(1), by applying the strain  $\varepsilon_j$  and calculating the corresponding stresses, The deformation matrix applied is

$$\mathbf{D} = \mathbf{I} + \boldsymbol{\varepsilon}, \quad (2)$$

where  $\mathbf{I}$  is the  $3 \times 3$  unit matrix, and  $\boldsymbol{\varepsilon}$  is the strain-matrix in Voigt notation. In the 3D case, the strain matrix is

$$\boldsymbol{\varepsilon} = \begin{bmatrix} \varepsilon_1 & \frac{\varepsilon_6}{2} & \frac{\varepsilon_5}{2} \\ \frac{\varepsilon_6}{2} & \varepsilon_2 & \frac{\varepsilon_4}{2} \\ \frac{\varepsilon_5}{2} & \frac{\varepsilon_4}{2} & \varepsilon_3 \end{bmatrix}. \quad (3)$$

The deformed crystal lattice vector is

$$\mathbf{A}' = \mathbf{A} \cdot \mathbf{D} \quad (4)$$

where  $\mathbf{A}$  is the crystal lattice vector without deformation.

### B. Elastic moduli and anisotropy

From the elastic constants, the elastic moduli can be readily derived. The Voigt and Reuss elastic moduli for different crystal systems are calculated according to Ref.<sup>15</sup>. According to the Voigt–Reuss–Hill approximations<sup>16</sup>, the arithmetic average of Voigt and Reuss bounds is

$$B = B_{\text{VRH}} = \frac{B_V + B_R}{2}, \quad (5)$$

and

$$G = G_{\text{VRH}} = \frac{G_V + G_R}{2} \quad (6)$$

respectively.

Young's modulus  $E$  is calculated by

$$E = \frac{9BG}{3B + G}, \quad (7)$$

and Poisson's ratio is

$$\nu = \frac{3B - 2G}{2(3B + G)}. \quad (8)$$

The elastic anisotropy is a direct reflect of spatial anisotropy of chemical bonding. Chung and Buessem defined an elastic anisotropy index<sup>17</sup>,

$$A^C = \frac{G_V - G_R}{G_V + G_R}. \quad (9)$$

Ranganathan and Ostoja-Starzewski proposed a more general anisotropy index called the universal elastic anisotropy index<sup>18</sup>,

$$A^U = 5 \frac{G_V}{G_R} - \frac{B_V}{C_R} - 6 \geq 0. \quad (10)$$

$A^U = 0$  corresponds to the locally isotropic crystals<sup>18</sup>.

### C. The calculation details of stress tensors

The crystal Ru has a hexagonal closely-packed (hcp) structure up to 600 GPa. Before the calculations of elastic constants, the crystal structure of Ru was first optimized within the framework of DFT at each pressure. Then the stress components were calculated accurately after atomic positions were relaxed under specific deformations applied according to our recently proposed "the optimized high efficiency strain-matrix sets (OHES)"<sup>13</sup>. The relaxations stopped after the forces acted on each atom were less than 0.02 eV/Å. The projector augmented wave (PAW) method<sup>19</sup> as implemented in the Vienna ab initio simulation package (VASP)<sup>20,21</sup> was adopted in all the structural optimizations and stress computations in this work. The Perdew, Becke and Ernzerhof (PBE)<sup>22</sup> generalized gradient approximation (GGA) was used for the exchange-correlation functional. The energy cutoff values were set to ensure energy to be converged to  $10^{-6}$  eV.

## III. RESULTS AND DISCUSSIONS

### A. Elastic constants

The calculated lattice parameters accords very well with both experimental and others' theoretical results, as shown in Table II. Also listed in Table II are our calculated elastic constants of Ru at 0 GPa. We see that our elastic constants are in reasonably good with experimental data and others' calculated results. Especially, we note that our stress-strain results are in very good agreement with the results from the energy-strain method by Lugovskoy et al.<sup>12</sup>. It is not surprising because they are the zero-pressure elastic constants, not considering pressure effects in both the stress-strain and energy-strain methods.

In order to compare the stress-strain method with the energy-strain method (Ref.<sup>12</sup>), we accurately tuned our pressures to correspond to those calculated in Ref.<sup>12</sup>. The maximum difference in pressure is not larger than 0.3

Table I. The comparison of our calculated high-pressure elastic constants of Ru with those from Ref.<sup>12</sup>. The atomic volume ( $V$ ) is in  $\text{\AA}^3$ , and pressure ( $P$ ) and elastic constants  $C_{ij}$  are in GPa.

	$V_0$ ( $\text{\AA}^3$ )	$a$ ( $\text{\AA}$ )	$c/a$	$C_{11}$	$C_{12}$	$C_{13}$	$C_{33}$	$C_{44}$	
	13.75	2.72	1.577	583.2	184.3	183.1	652.2	191.9	This work
	13.76	2.72	1.578	577.4	176.7	170.9	644.2	190.4	Calc. <sup>12</sup>
	13.24	2.68	1.584	701.0	196.2	187.4	774.5	240.0	Calc. <sup>23</sup>
				627.9	154.2	125.5	565.4	150.0	Calc. <sup>24</sup>
	13.51	2.70	1.585						Expt. <sup>25</sup>
	13.49	2.71	1.552						Expt. <sup>26</sup>
	14.48	2.71	1.582	576.3	187.2	167.3	640.5	189.1	Expt. <sup>27</sup>
$dC_{ij}/dP$				7.20	3.47	3.12	7.78	1.74	This work
				7.16	3.26	3.24	7.65	1.69	Calc. <sup>12</sup>
							1.67	1.67	Expt. <sup>25</sup>

Table II. The lattice parameters of Ru, in comparison with experimental data and others' theoretical values.

GPa, as shown in Table III. The corresponding mean atomic volumes are also in good agreement with each other. The maximum of mean atomic volume differences are not larger than  $0.04 \text{ \AA}^3$ , below 500 GPa. The high-pressure elastic constants are listed in Table III, from which we can numerically compare the elastic constants from the two different methods, the stress-strain and energy-strain methods. The pressure derivative of elastic constants  $dC_{ij}/dP$  are shown in Table II. It is surprisingly good that our stress-strain values agree with the energy-strain values that were calculated with complex pressure corrections by Lugovskoy et al.<sup>12</sup>. This indicates that, although the stress-strain method is rather straightforward to calculate the high-pressure elastic constants, it can reach the same accuracy of the energy-strain method with complicated pressure corrections.

To clearly compare the high-pressure elastic constants from the two methods, we presented all the elastic constants versus pressure data in Fig. 1. Except for the slight differences in  $C_{11}$  and  $C_{12}$  beyond 400 GPa, other elastic constants ( $C_{13}$ ,  $C_{33}$ , and  $C_{44}$ ) are in excellent agreement with each other for the two methods, in the whole pressure range from 0 up to  $\sim 600$  GPa. We also compare totally all the high-pressure elastic constants from the two methods in Fig. 2, from which we again find the satisfactory agreements between the stress-strain and energy-strain methods. In order to statistically evaluate the agreement of our results with the previous ones, we calculated the coefficient of determination  $R^2$  score<sup>28</sup> of present compared to previous results. The evaluated  $R^2 = 0.9982$ , implying an excellent agreement quantitatively.

### B. Elastic moduli and elastic anisotropy

From our high-pressure elastic constants, we calculated the bulk modulus  $B$ , shear modulus  $G$ , and Young's modulus  $E$  according to Eqs. (5), (6), and (8), respectively,

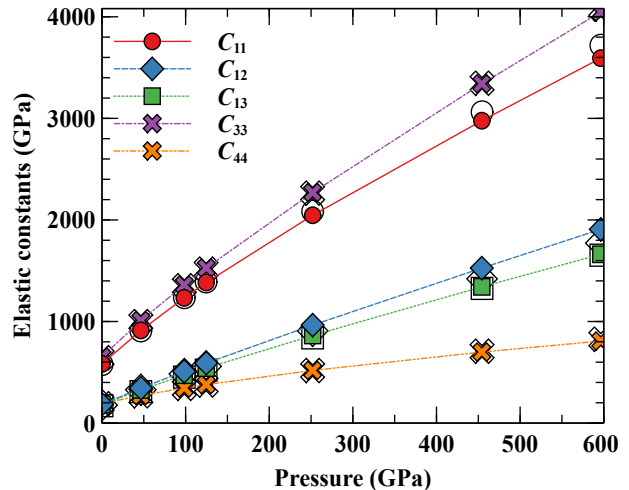


Figure 1. The calculated elastic constants of Ru versus pressure (solid symbols), in comparison with the calculated results from Ref.12 (open symbols).

and show them in Table. IV. These three elastic moduli all increase monotonously with pressure, implying the rigidity of Ru increases with pressure. We also calculated the Poisson's ratio of Ru and found that it increases from 0.2431 to 0.3367 at pressure ranging from 0 to  $\sim 600$  GPa.

In order to understand the variation of metallic bonding in Ru with pressure, we analyzed its elastic anisotropy properties. First, according to Eqs. (9) and (10), we calculated the elastic anisotropy indexes which can overall reflect the bonding characteristics of materials. As shown in Table IV, both  $A^U$  and  $A^C$  have very small variations at pressures from 0 up to  $\sim 600$  GPa. This indicates that the bonding properties keeps almost invariant in the hcp-Ru.

Second, we plotted the spatial variations of the Young's modulus, shear modulus, and Poisson's ratio at different pressures in Fig. 3. It can be clearly seen that the spatial

Table III. The comparison of our calculated high-pressure elastic constants of Ru with those from Ref.<sup>12</sup>. The atomic volume ( $V$ ) is in  $\text{\AA}^3$ , and pressure ( $P$ ) and elastic constants  $C_{ij}$  are in GPa.

	$V$	$P$	$C_{11}$	$C_{12}$	$C_{13}$	$C_{33}$	$C_{44}$
This work	12.30	46.5	912.4	344.1	326.9	1009.7	271.7
Ref. <sup>12</sup>	12.30	46.5	908.8	327.9	309.4	998.5	268.5
This work	11.29	98.3	1232.6	509.3	471.7	1360.0	345.2
Ref. <sup>12</sup>	11.31	98.5	1236.0	483.9	452.4	1352.0	341.8
This work	10.92	124.7	1384.0	590.1	542.0	1527.5	379.0
Ref. <sup>12</sup>	10.94	124.5	1391.0	558.9	521.2	1516.0	374.9
This work	9.66	251.9	2046.2	965.0	862.7	2269.8	518.4
Ref. <sup>12</sup>	9.69	251.9	2084.0	908.4	839.0	2264.0	517.5
This work	8.50	454.2	2977.1	1526.2	1341.4	3340.3	699.5
Ref. <sup>12</sup>	8.54	454.5	3063.0	1420.0	1326.0	3346.0	707.7
This work	7.96	596.5	3592.9	1908.0	1661.8	4047.7	807.9
Ref. <sup>12</sup>	8.10	596.5	3719.0	1772.0	1653.0	4081.0	825.8

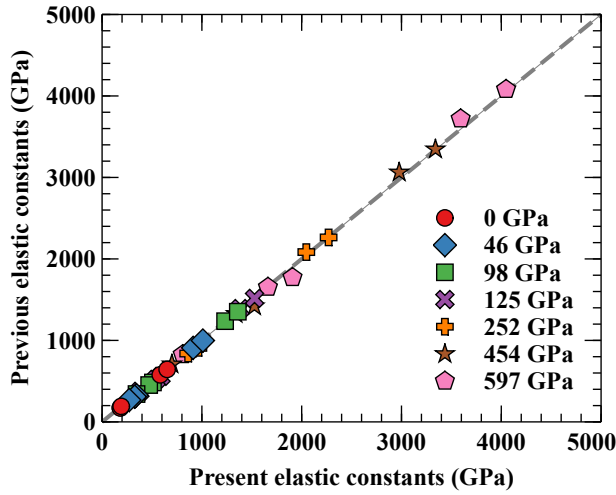


Figure 2. Comparison of the present calculated elastic constants and the previous results from Ref. 12.

elastic anisotropy of Ru almost remains unchanged with pressure. This accords well with the conclusion drawn from the elastic anisotropy indexes analysis.

Table IV. The high-pressure elastic moduli, Poisson's ratio, and elastic anisotropy indexes of Ru. The moduli are all in GPa.

$P$	$B$	$G$	$E$	$\nu$	$A^U$	$A^C$
0.0	324.	200.8	499.3	0.2431	0.0200	0.0018
46.5	536.3	287.2	731.2	0.2728	0.0266	0.0025
98.3	747.5	367.3	946.9	0.2889	0.0343	0.0033
124.7	849.0	404.3	1046.6	0.2945	0.0380	0.0037
251.9	1304.4	557.3	1463.4	0.3130	0.0553	0.0054
349.9	1632.0	658.1	1740.3	0.3223	0.0669	0.0066
454.2	1967.4	758.0	2015.2	0.3293	0.0792	0.0078
596.5	2410.0	883.4	2361.7	0.3367	0.0958	0.0094

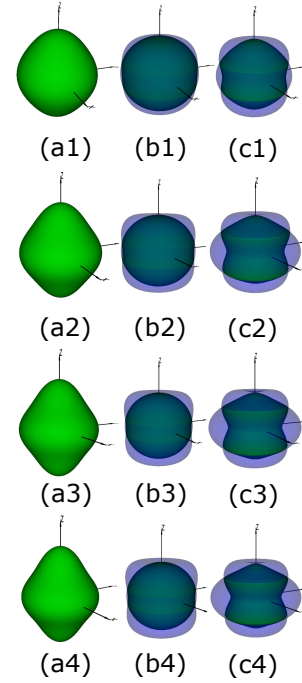


Figure 3. The spatial variations of the (a) Young's modulus, (b) shear modulus, and (c) Poisson's ratio of metal Ru at pressures (1) 0.03 GPa, (2) 251.9 GPa, (3) 454.2 GPa, and (4) 596.5 GPa, respectively.

### C. Sound velocity and Debye temperature

The phase velocity  $v$  and polarization of the three waves along a fixed propagation direction defined by the unit vector  $n_i$  are given by Christoffel equation,

$$(C_{ijkl}n_jn_k - \rho v^2\delta_{ij})u_i = 0, \quad (11)$$

where  $C_{ijkl}$  is the fourth-rank tensor description of the elastic constants,  $n$  is the propagation direction, and  $u$

the polarization vector.

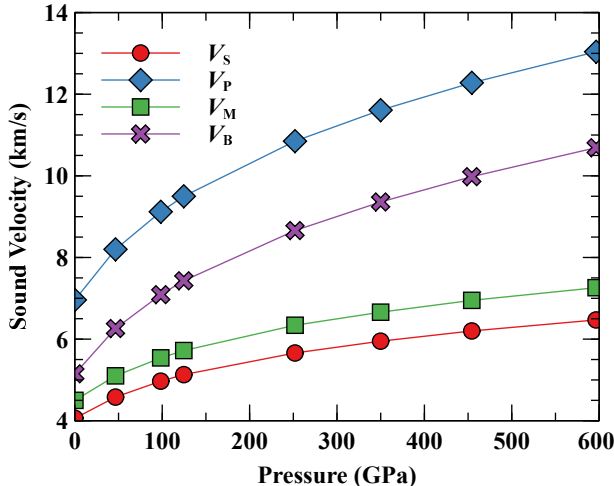


Figure 4. The sound velocities  $V_B$ ,  $V_P$ ,  $V_S$ , and  $V_M$  of metal Ru as functions of pressure.

Table V. The Debye temperatures of Ru at different pressure.

$P$ (GPa)	$\Theta_D$ (K)
0.0	444
46.5	522
98.3	584
124.7	609
251.9	703
349.9	756
454.2	804
596.5	859

The longitudinal wave velocity is

$$v_P = \sqrt{\frac{B + 4G/3}{\rho}}, \quad (12)$$

and the body wave velocity is

$$v_B = \sqrt{\frac{B}{\rho}}. \quad (13)$$

The shear wave velocity is calculated by

$$v_S = \sqrt{\frac{G}{\rho}}. \quad (14)$$

From  $v_S$  and  $v_P$ , we can obtain the mean wave velocity via

$$v_m = \left[ \frac{1}{3} \left( \frac{2}{v_S^3} + \frac{1}{v_P^3} \right) \right]^{-1/3}. \quad (15)$$

From the mean wave velocity data, we can calculate the Debye temperature from

$$\Theta_D = \frac{h}{k} \left[ \frac{3n}{4\pi} \left( \frac{N_A \rho}{M} \right) \right]^{1/3} v_m \quad (16)$$

where  $h$  is Planck's constant,  $k$  the Boltzmann's constant,  $N_A$  the Avogadro's number,  $n$  the number of atoms in the unit cell,  $M$  the weight of the unit cell, and  $\rho$  the density.

We show the calculated sound velocities in Fig. 4, from which we see the monotonous increases in all these sound velocities. This indirectly reflects the strengthening of the metallic bondings in Ru with increasing pressure.

Debye temperature  $\Theta_D$  corresponds to the temperature of a crystal's highest normal mode of lattice vibration, and it closely correlates the elastic properties with the thermodynamic properties<sup>29</sup>. The calculated Debye temperatures are listed in Table V. The increasing of  $\Theta_D$  with pressure again reflects the enhancing of the metallic bonding in Ru.

#### IV. CONCLUSIONS

In conclusion, we systematically compared the elastic constants of metal Ru calculated by the stress-strain method with those previously obtained by the energy-strain method. Both the zero-pressure and high-pressure elastic constants of Ru agree very well with each other for the two methods. But, our stress-strain method is much straightforward to implement to achieve high-pressure elastic constants. The energy-strain method depends on the complex pressure corrections for obtaining high-pressure elastic constants of materials, though the two methods can both reach the same accuracy. Thus the stress-strain method is more preferred for calculating the high-pressure elastic constants of materials. From the calculated elastic constants of Ru, we also analyzed the variations of its high-pressure elastic moduli, Poisson's ratio, elastic anisotropy, and Debye temperature with increasing pressure. All these physical parameters increases monotonously with pressure, implying the enhancement of rigidity of Ru under pressure. While, the elastic anisotropy varies slightly with pressure, reflecting the slight spatial variations of metallic bonding with pressure.

#### V. ACKNOWLEDGMENTS

We acknowledge the supports from the National Natural Science Foundation of China (41574076), the Key Research Scheme of Henan Universities (18A140024), the Key Laboratory of the Electromagnetic Transformation and Detection of Henan province, and the Research Scheme of LYNU Innovative Team under Grant No. B20141679.

- \* zl.liu@163.com  
† wanghy@hpu.edu.cn
- <sup>1</sup> A. M. Tehrani and J. Brgoch, *J. Solid State Chem.* **271**, 47 (2019).
  - <sup>2</sup> R. Golesorkhtabar, P. Pavone, J. Spitaler, P. Puschnig, and C. Draxl, *Comput. Phys. Commun.* **184**, 1861 (2013).
  - <sup>3</sup> N. W. Ashcroft and N. D. Mermin, *Solid State Physics* (Harcourt College Publishers, New York, 1976).
  - <sup>4</sup> P. Blanchfield and G. A. Saunders, *Journal of Physics C: Solid State Physics* **12**, 4673 (1979).
  - <sup>5</sup> G. V. Sinko and N. A. Smirnov, *J. Phys.: Condens. Matter* **14**, 6989 (2002).
  - <sup>6</sup> G. V. Sin'ko and N. A. Smirnov, *Phys. Rev. B* **71**, 214108 (2005).
  - <sup>7</sup> G. V. Sin'ko, *Phys. Rev. B* **77**, 104118 (2008).
  - <sup>8</sup> W. F. Perger, J. Criswell, B. Civalleri, and R. Dovesi, *Comput. Phys. Commun.* **180**, 1753 (2009).
  - <sup>9</sup> V. Wang, N. Xu, J. C. Liu, G. Tang, and W. T. Geng, "VaspkIt: A pre- and post-processing program for vasp code (arxiv:1908.08269v2)," (2019), arXiv:1908.08269.
  - <sup>10</sup> R. Yu, J. Zhu, and H. Q. Ye, *Comput. Phys. Commun.* **181**, 671 (2010).
  - <sup>11</sup> X. L. Zhang, Y. X. Han, H. Jia, N. Qu, and Z. L. Liu, *Commun. Theor. Phys.* **69**, 735 (2018).
  - <sup>12</sup> A. V. Lugovskoy, M. P. Belov, O. M. Krasilnikov, and Y. K. Vekilov, *J. Appl. Phys.* **116**, 103507 (2014).
  - <sup>13</sup> Z. L. Liu, "High-efficiency calculation of elastic constants enhanced by the optimized strain-matrix sets," (2020), arXiv:2002.00005.
  - <sup>14</sup> Z. L. Liu, "Elastool: An automated toolkit for elastic constants calculation," (2020), arXiv:2002.06535.
  - <sup>15</sup> Z. J. Wu, E. J. Zhao, H. P. Xiang, X. F. Hao, X. J. Liu, and J. Meng, *Phys. Rev. B* **76**, 054115 (2007).
  - <sup>16</sup> R. Hill, *Proc. Phys. Soc. London*, 350 **65**.
  - <sup>17</sup> D. H. Chung and W. R. Buessem, *J. of Appl. Phys.* **38**.
  - <sup>18</sup> S. I. Ranganathan and M. Ostoja-Starzewski, *Phys. Rev. Lett.* **101**, 055504 (2008).
  - <sup>19</sup> P. E. Blöchl, *Phys. Rev. B* **50**, 17953 (1994).
  - <sup>20</sup> G. Kresse and D. Joubert, *Phys. Rev. B* **59**, 1758 (1999).
  - <sup>21</sup> G. Kresse and J. Furthmüller, *Phys. Rev. B* **54**, 11169 (1996).
  - <sup>22</sup> J. P. Perdew, K. Burke, and M. Ernzerhof, *Phys. Rev. Lett.* **78**, 1396 (1997).
  - <sup>23</sup> L. Fast, J. M. Wills, B. Johansson, and O. Eriksson, *Phys. Rev. B* **51**, 17431 (1995).
  - <sup>24</sup> D. K. Pandey, D. Singh, and P. K. Yadawa, *Platinum Met. Rev.* **53**, 91 (2009).
  - <sup>25</sup> H. Olijnyk, A. P. Jephcoat, and K. Refson, *Europhys. Lett.* **53**, 504 (2001).
  - <sup>26</sup> C. Kittel, *Introduction to Solid State Physics* (John Wiley and Sons, Moscow, 1956).
  - <sup>27</sup> M. Dirts, A. Dirts, P. Budberg, and N. Kuznetsov, *Properties of Elements* (Ore and Metals PH, Moscow, 2003).
  - <sup>28</sup> [https://en.wikipedia.org/wiki/Coefficient\\_of\\_determination](https://en.wikipedia.org/wiki/Coefficient_of_determination).
  - <sup>29</sup> X. Luo and B. Wang, *J. Appl. Phys.* **104**, 073518 (2008).